Optimization of in-depth water diversion using a fully implicit thermal-compositional approach

Sangers, M.; Trujillo, R.; Voskov, D.; Leeuwenburgh, O.

DOI
10.3997/2214-4609.201802265

Publication date
2018

Document Version
Final published version

Published in
16th European Conference on the Mathematics of Oil Recovery, ECMOR 2018

We A1 13

Optimization Of In-Depth Water Diversion Using A Fully Implicit Thermal-Compositional Approach

M. Sangers* (TU Delft), R. Trujillo (TU Delft), D. Voskov (Stanford University and TU Delft), O. Leeuwenburgh (TNO and TU Delft)

Summary

We investigate the potential for improved recovery of subsurface energy resources (hydrocarbons or heat) through in-depth diversion technology. A number of pilot studies in the North Sea have demonstrated in recent years that sodium silicate can be used to block preferential flow paths and divert water to previously unswept areas of a reservoir. Accompanying simulation studies based on an explicit weak coupling of a reservoir flow simulator and an external chemical module have attempted to replicate the observed behaviour. Since the development of silicate gels and the accompanying permeability reduction is essentially a coupled flow-chemical process, we first will present a fully implicit compositional-reactive flow and transport implementation and investigate the impact of the grid and time-stepping resolution on simulation performance in 2D subsurface reservoirs mimicking petroleum and geothermal applications. We proceed to investigate the sensitivity of the recovery to design parameters of the in-depth diversion strategy. Since adjoint gradients are not typically available for these parameters and uncertainties associated with an application of in-depth divergence are large, we use an ensemble-based methodology to perform an optimization study. This study aims to find optimal strategies for combined waterflooding and design of in-depth diversion under geological uncertainty. It is demonstrated that in-depth diversion can significantly extend the life-time of hydrocarbon or geothermal fields when the timing of injection and the size of the sodium silicate batch is optimized. Finally, we discuss methods that help to address an issue of computational cost associated with the high resolution required for accurate simulation of the coupled process.

Introduction

Many conventional waterflooded reservoirs are reaching their end of life with a lot of production wells producing at high water cut. Newly discovered reservoirs tend to be more complex, and therefore carry more risk and relatively high development costs. As a result, there is increased interest in Enhanced Oil Recovery (EOR) and Improved Oil Recovery (IOR) methods that can be used to extend the operating life of existing fields and increase the ultimate recovery at reasonable cost.

During waterflooding the water will tend to follow the pathway of least resistance. It may therefore predominantly flow through high permeable zones and channels, leaving other reservoir areas unswept. One option to improve the volumetric sweep efficiency is the use of IOR methods such as in-depth water divergence (IDD). Green chemicals, such as the PLONOR listed chemical sodium silicate (Hatzignatiou et al. (2016)), should make these methods more attractive for wide-scale employment. Sodium silicate can potentially flow for a long distance, far away from the injector, to a place where it forms a gel under certain activation conditions, either thermal or chemical. As such a gel has the ability to withstand large pressure gradients it can divert injected water to unswept zones (Trujillo et al. (2018)).

A number of pilot studies in the North Sea have demonstrated in recent years that sodium silicate can be successfully employed to enhance recovery from producing fields (Skrettingland et al. (2012, 2014)). Combined with these pilots, experimental laboratory work has given insight on activation conditions, core-scale behaviour, and chemistry of the poorly understood polymerization process (Icopini et al. (2005); Stavland et al. (2011)). Several numerical simulation studies, based on a weak coupling of a reservoir flow modeling and a separate software module for chemical reactions, have been able to replicate the main characteristics of the observed behaviour (Hiorth et al. (2016); Skrettingland et al. (2014)). Since the development of silicate gels and the accompanying permeability reduction is essentially a coupled process, Trujillo et al. (2018) recently proposed a fully implicit coupled chemical-compositional-flow implementation.

The success of an IDD process depends on complex interactions between multiple parameters, and only some of them are under the control of an operator. As the first stage of the IDD process a pre-slush volume of Potassium Chloride (KCL) brine is injected to act as a stabilizer, preventing clay swelling and rapid plugging due to mineral precipitation (Skrettingland et al. (2014)). The operator can furthermore control the timing and duration (or volume) of the sodium silicate slug, and the concentration of the solution. Other aspects of the IDD process are more complex to control or poorly understood. Stavland et al. (2011) mention the pH changes within the reservoir due to the complex chemical reactions taking place. Low pH can result in a short gelation time and therefore alkaline gels are preferred over acidic gels, despite having a lower gel strength (Hamouda and Amiri (2014)). Additionally Trujillo (2017) indicates that the particle size is a key parameter in the reduction of porosity and permeability, where the Icopini et al. (2005) reaction model with low concentration rates is the best suitable for simulation purposes.

The resulting difficulty of designing a good operational strategy suggests that optimization methods can help identifying a good (or even optimal) strategy. To the best of our knowledge, optimization of IDD involving tuning of the silica injection parameters and treatment of upscaling effects in reactive transport has not previously been performed. Here we intend to investigate if such a model-based approach could be feasible.

There are some challenges related to the correct simulation of the gelation process. Trujillo et al. (2018) mention the scale dependence of the kinetic rate. The physics of the silica reaction kinetics occur in the local domain and much faster than the transport phenomena in the global domain. The high order reaction rate of concentration suggests the need for upscaling this complexity. A proper choice for the simulation scale parameters will therefore contribute to the performance of any optimization exercise.

In this study, we therefore focus on the impact of the spatial and temporal resolution of the simulations, and on the potential to use the simulations to find operational IDD strategies (timing, duration and

concentration of the sodium silicate solution slug) that deliver improved performance over conventional waterflooding strategies. For enhanced realism we will consider the presence of geological uncertainty and use an ensemble of geological realizations to represent this uncertainty. We demonstrate that the resulting optimal strategy is non-trivial and differs from a normal reactive approach, where the injection is started immediately after water breakthrough.

This remainder of this paper starts with a discussion of the modeling approach and a brief description of the IDD simulation process. Subsequently we describe the optimization formulation based on an ensemble approach. Several numerical experiments are presented based on a simple 2D model representing a layered vertical reservoir cross-section connecting an injection and production well. We present results on the sensitivity to model parameters and applications of an optimization methodology to both deterministic and stochastic models, and end with some conclusions.

Modeling approach

In-depth water diversion simulation

In this section, we briefly describe the major ingredients of the modeling approach used for this study. For further details of the implementation the reader is referred to Trujillo et al. (2018). Trujillo et al. (2018) adapted and validated the Hiorth et al. (2016) porosity-permeability model and the 4-component silica gelation reaction suggested by Icopini et al. (2005) for in-depth divergence simulation. These models were implemented in the Automatic Differentiation General Purpose Research Simulator (AD-GPRS) developed at Stanford University (Voskov and Tchelepi, 2012; Zaydullin et al., 2014; Garipov et al., 2018). The governing equations for reactive flow and transport, as implemented in ADGPRS (Farshidi et al., 2013; Voskov et al., 2017), involve generic conservation of mass of species

$$\frac{\partial n_i}{\partial t} + l_c + q_c = \sum_{k=1}^{K} v_{ck} r_k + \sum_{q=1}^{Q} v_{cq} r_q, \quad c = 1, \ldots, C, \tag{1}$$

where n_c is the overall mass of component, l_c is the total flux associated with that component, v_{ck} is the stoichiometric coefficient associated with kinetic reaction k for the component c and v_{cq} is the stoichiometric coefficient associated with equilibrium reaction q for component c. r_k is the rate for kinetic reaction k and r_q is the rate for equilibrium reaction q. In this study, we only include kinetic reactions to describe the gelation process as suggested in Trujillo et al. (2018). All equilibrium reactions are neglected

In this study we assume solid species of the reaction are not transported, but deposited as a gel within the matrix, changing porosity. As mentioned earlier, the 4-component reaction for modeling the polymerization process is used (Trujillo et al., 2018),

$$H_8Si_3O_{10(\mathrm{aq})} + H_4\mathrm{Si}O_{4(\mathrm{aq})} \xrightarrow{k_1} H_8Si_4O_{12(\mathrm{gel})} + 2H_2O \tag{2}$$

Icopini et al. (2005) reported a fourth order reaction rate (3) of the concentration for the consumption of H_4SiO_4.

$$\frac{dc}{dt} = -k\,c^4 \quad , \tag{3}$$

where c is the concentration of $H_4\mathrm{Si}O_{4(\mathrm{aq})}$. The change of porosity is related to the molar deposition of the solid species according to

$$\phi(t) = 1 - C_{rock} - \frac{N_{solid}(t) \times M_{v_{solid}}}{V_{cell}} \quad . \tag{4}$$

where N_{solids} is the amount of moles of solids deposited, $M_{v_{solid}}$ is the molecular volume of the solid, V_{cell} the cell volume, and C_{rock} the fraction of rock. Finally, the Hiorth et al. (2016) pore throat blockage

model (5) approximates permeability as function of initial permeability k_0 and porosity φ_0, the mass fraction of deposited silica over water Y and the water saturation S_w,

$$k = k_o \left(1 + 275 Y S_w \sqrt[2]{\frac{k_o}{\phi_o}}\right)^{-2} . \tag{5}$$

Optimization formulation

The primary objective in the exploitation of oil reservoirs is normally to maximize economic value, where value is generally dominated by the revenues associated with increased oil recovery. One way to improve oil recovery is to implement smart injection and production strategies. Such strategies can be found with the help of simulation models and numerical optimization techniques. A waterflood strategy, for example, is characterized by time series of injection and production rates, or bottom hole pressures, in all wells. These so-called controls can be manipulated such that a user-specified objective function, that can be evaluated from the model output, is maximized.

When IDD is implemented to further increase recovery, an additional set of controls should be included. Here, we will consider the start time for the injection of the silicate slug, the slug size, and the silicate concentration as the control variables. In this study, the slug size will be defined in terms of the injection duration in days. In order to determine the economic value of the project, we will define the objective function to be net present value (NPV) which is computed as the integral over all timesteps $n = \{1,\ldots,N\}$ of the discounted cash flow incurred in each time step.

This cash flow is obtained as the product of production and injection rates of oil (Q_o), water (Q_{wi} and Q_{wp}) and silicate (Q_c) with the associated prices per unit volumes (r_o, r_{wi}, r_{wp}, and r_c) respectively, and the time step interval Δt. The subscript o stands for oil, wi for water injected, wp for water produced, and c for the injected sodium silicate. The discount factor b per time interval τ is used to include the time value of money. With these definitions the objective function becomes

$$J = \sum_{k=1}^{K} \left[\frac{(Q_o \cdot r_o - Q_{wp} \cdot r_{wp} - Q_{wi} \cdot r_{wi} - Q_c \cdot r_c) \cdot \Delta t}{(1+b)^{(t/\tau)}} \right]. \tag{6}$$

The values of the fixed prices that are used in this study are listed in Table 1.

Notation	Value	Unit
r_o	150	$\$/m^3$
r_{wp}	25	$\$/m^3$
r_{wi}	5	$\$/m^3$
b	0 and 8	%/year

Table 1 *Prices per injected or produced volume and discount rate used in this paper.*

The cost of the injected silicate solution r_{ci} is expressed as a function of the silicate concentration in water (7). With C being the concentration in wt% and P the price of dry sodium metasilicate in $\$/m^3$, the cost per unit volume of concentrate is

$$r_{ci} = P \cdot \frac{C}{100} + r_{wi} \cdot \frac{100 - C}{100}. \tag{7}$$

Mayer et al. (1983) reported a price range of 310 - 415 USD per dry ton sodium metasilicate (Na_2SiO_3, 2.4 g/cm^3), equivalent to $P = 820$ USD per m^3. For the simple cases considered in this work, this price range could be on the high side, leading to a suboptimal strategy. Therefore, lower ranges for P will be considered.

Ensemble optimization of in-depth water diversion

Maximization of the objective function is an iterative process in which incremental adjustments of the control values are proposed in each iteration that should provide a consistent increase of the objective function. An efficient way to achieve this is to exploit the objective function gradient, which contains the sensitivities of objective function with respect to all controls. For cases in which no exact gradients are available, which is very likely to be the case for the controls describing the IDD process, approximate gradients or global search methods need to be employed. If the model is uncertain, as in the case of oil production, ensemble-based approximate gradients methods have been found to be efficient. This method was originally suggested by Chen et al. (2009) and later improved by Fonseca et al. (2014). Here, we present only a brief description. For more details the reader may refer to Fonseca et al. (2017).

The controls are gathered in a vector $\boldsymbol{u}$ of length n. If the control vector consists of time series of well rates or pressures for all wells, n may be very large. Here we will focus only on demonstrating the use of ensemble optimization for optimization of IDD strategies, and we will therefore only consider a single injection well with concentration, timing and duration of silicate injection as controls (i.e. $n = 3$)

$$\boldsymbol{u} = [u_{\text{concentration}}, u_{\text{timing}}, u_{\text{duration}}]. \tag{8}$$

Figure 1 illustrates the general injection strategy including the controls, where u_{timing} is given by t_0 and u_{duration} by Δt. The blue color indicates water injection (zero silicate concentration), while the green color indicates a non-zero silicate concentration. We will consider constant injection rates in this study, but this simplification can easily be relaxed, adding separate rate controls for each time interval.

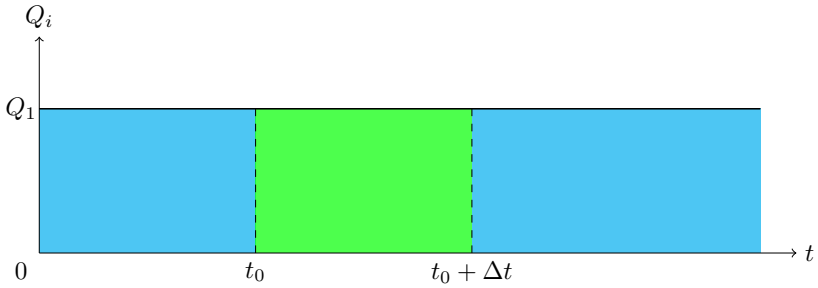

Figure 1 *Sodium silicate injection with a constant injection rate.*

In each optimization iteration k, an ensemble of control vectors is created by perturbation of the current control solution and stored in the matrix U. The perturbed control vector $\hat{\boldsymbol{u}}_k$ and the unperturbed control vector $\boldsymbol{u}_k$ both have length n. Each perturbed control is used as input for a model simulation, resulting in a perturbed objective function value $J(\hat{\boldsymbol{u}}_k^i)$, where $i = \{1, \ldots, m\}$ with m the ensemble size. Objective function anomalies, constructed as the difference with the objective function for the unperturbed controls, are then stored in vector $\boldsymbol{j}$. The two ensemble matrices are thus defined as

$$\boldsymbol{U} = \left[\hat{\boldsymbol{u}}_k^1 - \boldsymbol{u}_k \quad \hat{\boldsymbol{u}}_k^2 - \boldsymbol{u}_k \quad \ldots \quad \hat{\boldsymbol{u}}_k^m - \boldsymbol{u}_k\right], \tag{9}$$

and

$$\boldsymbol{j} = \left[J\left(\hat{\boldsymbol{u}}_k^1\right) - J\left(\boldsymbol{u}_k\right) \quad J\left(\hat{\boldsymbol{u}}_k^2\right) - J\left(\boldsymbol{u}_k\right) \quad \ldots \quad J(\hat{\boldsymbol{u}}_k^{N_p}) - J\left(\boldsymbol{u}_k\right)\right]^T. \tag{10}$$

Normally the number of perturbations is smaller than the number of control variables ($m < n$). The system of equations is then underdetermined and the gradient can be evaluated using the generalized inverse (11),

$$\boldsymbol{g} = (\boldsymbol{U}^T \boldsymbol{U})^+ \boldsymbol{U}^T \boldsymbol{j} \tag{11}$$

If the model is uncertain, an ensemble of m model realizations can be used. In that case, the unperturbed controls can be applied to all model realizations to compute an expected objective function value. In the above equations, we may then replace the terms $J(\boldsymbol{u}_k^i) - J(\boldsymbol{u}_k)$ by $J(\boldsymbol{u}_k^i, \boldsymbol{p}^i) - J(\boldsymbol{u}_k, \boldsymbol{p}^i)$ where $\boldsymbol{p}^i$ is the parameter vector for realization i (see Fonseca et al. (2014) and Fonseca et al. (2017) for details). We refer to such optimization under uncertainty as the robust optimization.

In this study, a simple trust region optimization scheme is used to update the controls with the gradient information to maximize objective function value. The trust region method makes use of a model function f that approximates the behaviour of the objective function near the point $\boldsymbol{u}_k$. For the model, we will use the first order Taylor expansion of the objective function around $\boldsymbol{u}_k$, and look for a control update $\boldsymbol{u}_k + \boldsymbol{s}$ that lies inside the trust region,

$$\max_{\boldsymbol{s}} f(\boldsymbol{u}_k + \boldsymbol{s}) = \max_{\boldsymbol{s}} J(\boldsymbol{u}_k + \boldsymbol{s}) = J(\boldsymbol{u}_k) + \boldsymbol{g}_k^T \boldsymbol{s} \tag{12}$$

$$\text{s.t. } ||\boldsymbol{s}||_\infty < \tau \cdot (\boldsymbol{u}^{\max} - \boldsymbol{u}^{\min}) \quad \text{and} \quad \boldsymbol{u}^{\min} \leq \boldsymbol{u}_k \leq \boldsymbol{u}^{\max}, \tag{13}$$

where τ is the trust region size. The gradient is susceptible to noisy and small gradient components. To reduce this effect, the trust step is reset to zero if component g_i is close to zero.

$$s_i = \begin{cases} \min\left[\left(u_i^{\max} - u_i\right), \tau\left(u_i^{\max} - u_i^{\min}\right)\right] & \text{if } g_i > 0 \\ \max\left[\left(u_i^{\min} - u_i\right), -\tau\left(u_i^{\max} - u_i^{\min}\right)\right] & \text{if } g_i < 0 \\ 0 & \text{if } g_i = 0. \end{cases} \tag{14}$$

If the original search direction is positive, then the new search direction will be the minimum of the distance to the bounds, and the trust-size factor should be multiplied by the difference between the maximum and the minimum of the control. If it is negative, then it will be the maximum. A standard trust size update scheme is applied to increase or decrease the trust region size based on the improvement in the objective function.

Numerical results

In this section, we describe the simulation setup and investigate its sensitivity to the model parameters. Next, we will apply optimization for deterministic and stochastic models.

2D layered model

A simple 2D model will be used to test our workflow for IDD optimization. The model represents a vertical reservoir cross section connecting a vertical injector, positioned on one end, and a a vertical producer on the opposite end. We consider different geological scenarios for the location of one or more high-permeable layers that provide a preferred pathway for injected water. In the first scenario, a single layer with a permeability of 400 mD connects injector and producer in the middle of the domain. The remaining background area has a much lower permeability of 50 mD. Additional parameters are listed in Table 2.

Property	Value
Δx, Δy, Δz	1 m, 100 m, 20 m
dimensions	256, 1, 5
$k_{background}$	50 mD (layers 1, 2, 4 and 5)
$k_{channel}$	400 mD (layer 3)
ϕ	0.2
Q_{inj}	564 m^3/day
BHP_{prd}	390 bar

Table 2 *Parameters of the 2D model and waterflooding strategy as used in the first numerical experiments.*

A base case recovery strategy is defined for the reference as a conventional waterflooding, i.e. without implementation of sodium silicate injection. The instantaneous and cumulative oil production rates for the base case strategy are indicated by the dashed lines in Figure 2 and Figure 3 respectively.

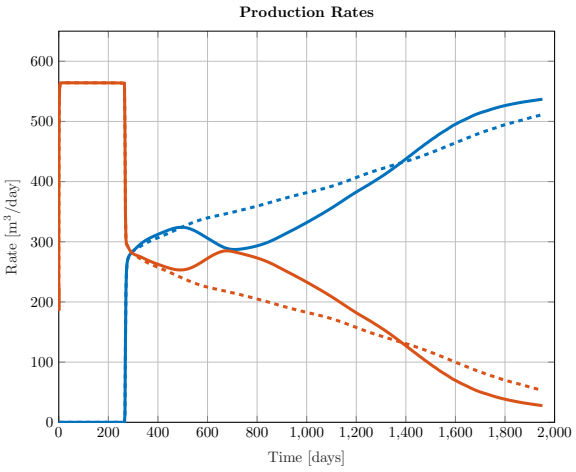

Figure 2 *Rates: oil (red), water (blue). With sili-cate (solid) or without (dashed).*

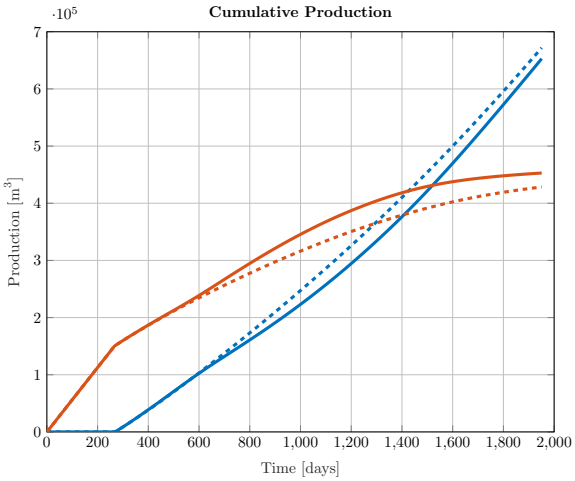

Figure 3 *Cumulatives: oil (red), water (blue). With silicate (solid) or without (dashed).*

After approximately 260 days water breaks through in the producing well. After 2000 days, oil production has significantly decreased and the water cut has increased to a level that would make further production uneconomic. A reasonable reactive approach might be to start sodium silicate injection after water breakthrough. A 4wt% silicate solution was injected for 350 days, resulting in a total slug volume of 200,000 m^3 and a permeability reduction of 80% (Figure 4). This strategy is indicated by the solid line in Figure 2 and Figure 3.

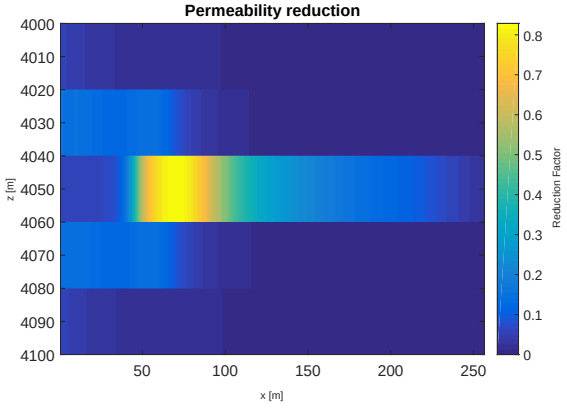

Figure 4 *Permeability reduction factor (color scale).*

Even though the plug permeability (around 70 mD) is still higher compared to the background permeability (by about 20 mD), there is diversion of water visible around the plug (Figure 4). The resulting incremental oil production relative to the base strategy is 5.7%.

Sensitivity to resolution

Before attempting to find optimal strategies for IDD, we first investigate the sensitivity of simulations results to the spatial and temporal resolution for simulation of the IDD process. If sensitivity is large, we need to perform simulations at very high spatial and temporal resolution that makes practical optimization infeasible for larger and more realistic models.

Simulations for different resolutions of grid cell size Δx were performed with a fixed time step of 2 days (Figure 5). Figure 6 shows the relative error in the oil production rate for the tested spatial resolutions. The error in production increases around the time of water breakthrough and towards the end of the production period. Figure 5 however suggests that rate errors are relatively moderate in absolute terms and that the highest relative errors occur when absolute rates are low, and should not strongly affect the total recovery.

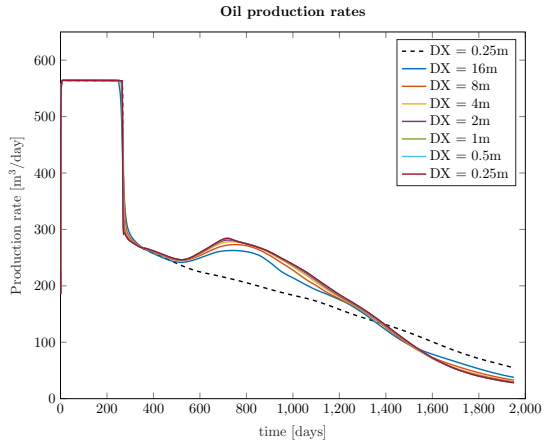

Figure 5 *Oil production rates for varying spatial grid resolution.*

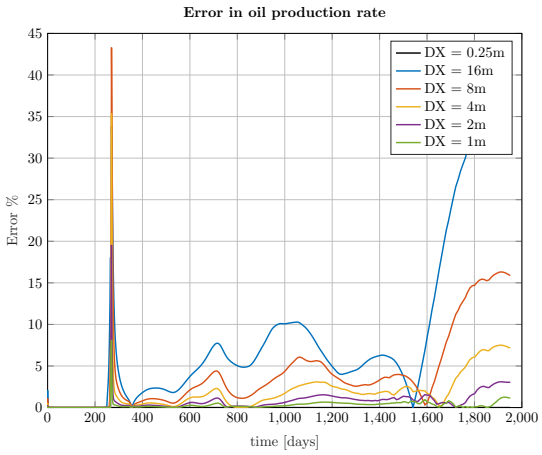

Figure 6 *Error in oil production rate for varying spatial grid resolution.*

This is confirmed by Figure 7 and Figure 8 that show both the sensitivity of oil recovery and permeability reduction to spatial and temporal resolution. Both quantities are affected by less than around 2% for the considered ranges of scales.

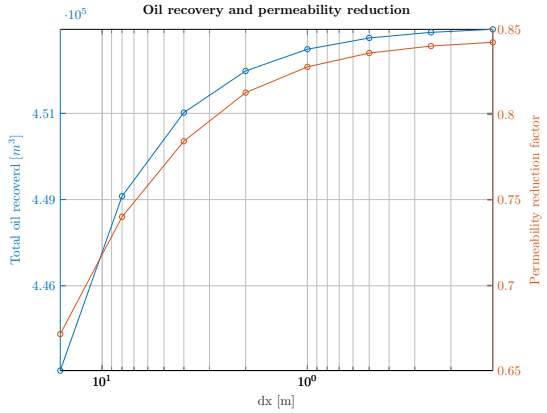

Figure 7 *Cumulative oil recovery and permeability reduction as a function of grid resolution for $\Delta t = 1$ day.*

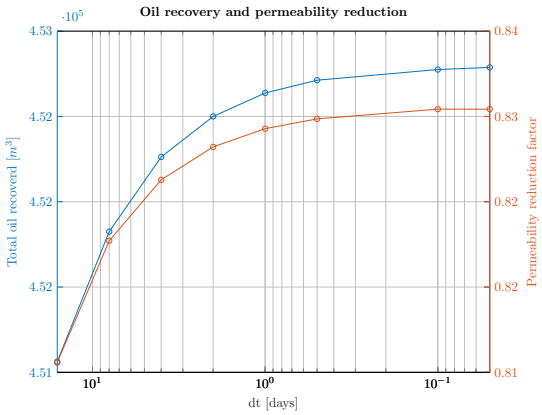

Figure 8 *Cumulative oil recovery and permeability reduction as a function of time resolution for $\Delta x = 1$ m.*

Further illustrations of the effect of spatial and temporal resolution are shown in Figure 9 to Figure 12 which consider the location of plug forming and the effect of resolution in simulation time. The distance from the injector to the plug was taken at the cell location with the maximum amount of precipitate. Figure 9 and Figure 10 show a decreasing distance for higher resolution. Total simulation time increases rapidly for spatial scales below $\Delta x = 1$ m.

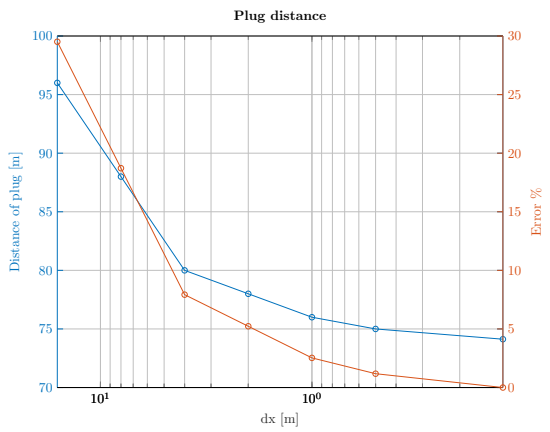

Figure 9 *Distance of plug from injector as a function of grid resolution for $\Delta t = 1$ day.*

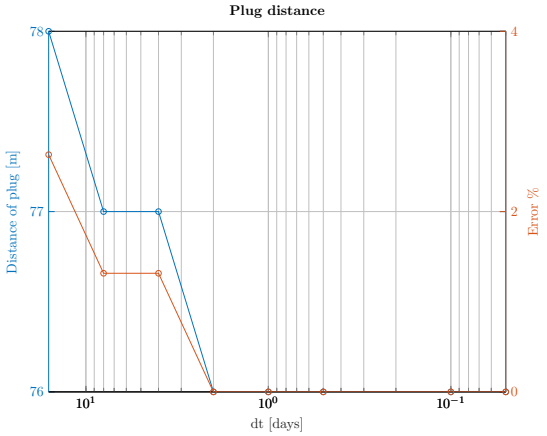

Figure 10 *Distance of plug from injector as a function of time resolution for $\Delta x = 1$ m.*

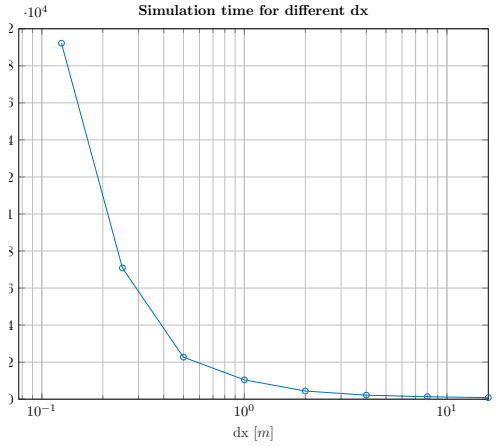

Figure 11 *Simulation time as a function of Δx. Resolution in time is $\Delta t = 1$ day.*

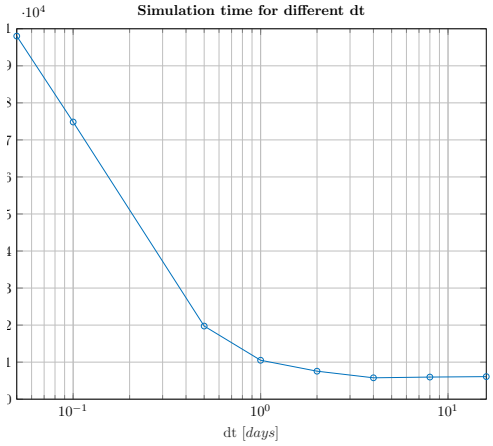

Figure 12 *Simulation time as a function of Δt. Resolution in space is $\Delta x = 1$ m.*

Based on the results from the sensitivity experiments, we conclude that a relatively coarser grid (than $\Delta x = 1$ m) and relatively larger time steps (than $\Delta t = 1$ days) are acceptable for forward simulation.

Case 1. Deterministic optimization for a single high-permeable layer

A deterministic optimization (single model realization) with both silicate solution injection timing t_0 and duration Δt as controls was performed for the 2D model, with a fixed concentration of 4wt% and a price of sodium silicate $r_{ci} = 17$ USD/m^3. Undiscounted cash flow was used as the objective function. To verify the results of the optimization, we first conducted an exhaustive search by evaluating multiple combinations of these two control parameters (Figure 13). The optimum was found for $[t0, \Delta t] = [200, 150]$. Next, an ensemble-based optimization was performed with an initial control combination of $[t0, \Delta t] = [1400, 550]$. The optimization process is indicated by the arrows in Figure 13 where every green point corresponds to a control update. The red dot is the end result of the optimization and

this optimum was found at $[t0, \Delta t] = [176, 136]$ with an NPV of $4.5174 \cdot 10^7$ USD which is very close to the highest value found by exhaustive search.

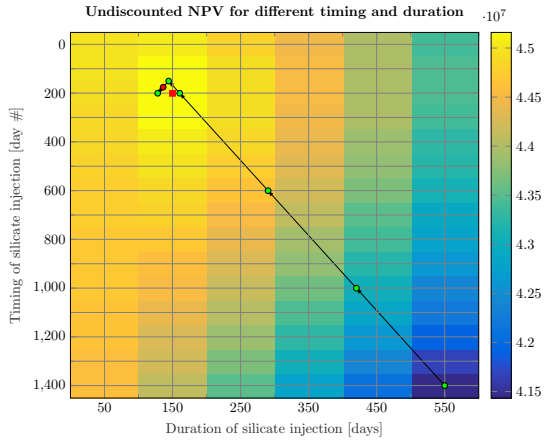

Figure 13 *Undiscounted J (color scale) and control updates (arrows and points) resulting from deterministic optimization.*

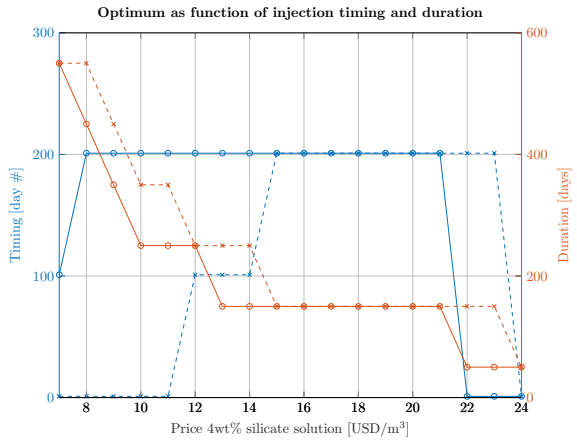

Figure 14 *Optimal control strategies for optimization of undiscounted (solid) and discounted (dashed) NPV.*

Since the optimum depends largely on the silicate solution price, Figure 14 shows the optimum combinations of $[t0, \Delta t]$ as function of price for both undiscounted and 8% discounted NPV, where $t_0 \in [0, 1400]$ and $\Delta t \in [50, 550]$. The strategy is similar for the price of sodium silicate between 15 and 21 USD/m^3, but between 8 and 15 USD/m^3 the discounted case benefits from injecting earlier.

Case 2. Deterministic optimization for a heterogeneous reservoir

Up to now, we consider the known presence of a single high-permeabile layer connecting the injector and producer wells. In reality, we may encounter situations with different, mostly uncertain, geology. Since in that case we cannot construct a model that is a perfect representation of the subsurface, we may choose to construct an ensemble of models that all are equally probable as the description of the subsurface reservoir. It may be expected that each geological scenario would result in a different response of the subsurface system to the same control strategy.

In order to test this assumption, we consider a slight modification of our original setup. It is assumed that high-permeable layers are present in the reservoir that create a partial connection between the two wells. The layers are disconnected in the middle part of the reservoir cross-section. We also assume that the reservoir contains additional high-permeable features with only approximately known extensions in lateral distance, representing for example, channel beds.

One of such scenarios is shown in Figure 15. In this model, $K_x = K_y$ and $K_z = {}^1/_{10} \cdot K_x$ and $K_x = 1000$ mD in the high permeable features, and K_x is either 50 or 1 mD in the low-permeable parts of the reservoir. The size of the model is 200m x 100m x 100m with grid dimensions of 1m x 100m x 10m and uniform porosity of 0.2. First a normal waterflood was performed. After 2000 days with an injection rate of 500 m^3/day and producer BHP of 390 bar, there are 3 areas visible with high remaining oil saturation (Figure 16). The NPV, predicted with this waterflood strategy, is \$14 millions.

Optimizations were performed with different prices P for dry sodium metasilicate (equation 7) where we add the silicate concentration as a third control. We report here the results obtained with a value of $P = 100$ \$/m^3 for which the optimal strategy achieves an undiscounted NPV of \$23 million, which represents a 64% increase over the waterflood scenario. The optimal strategy is to inject water for 438 days before starting injection of a 7.44 wt% silicate solution for 744 days ($[t, \Delta t, C] = [438, 744, 7.44]$). Since the injection rate is fixed at 500 m^3/day, the total volume of injected silicate solution is 372,000

m^3. The plug was formed 90 meters away from the injector, as indicated by the red circle in Figure 17. At this location, the largest permeability reduction was observed.

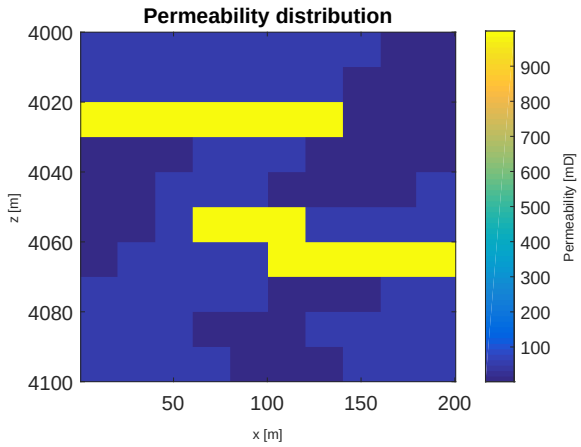

Figure 15 *Permeability K_x..*

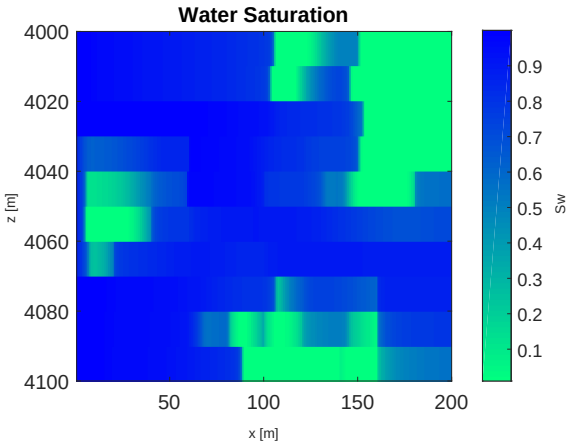

Figure 16 *Water saturation at the end of the water-flood reference strategy.*

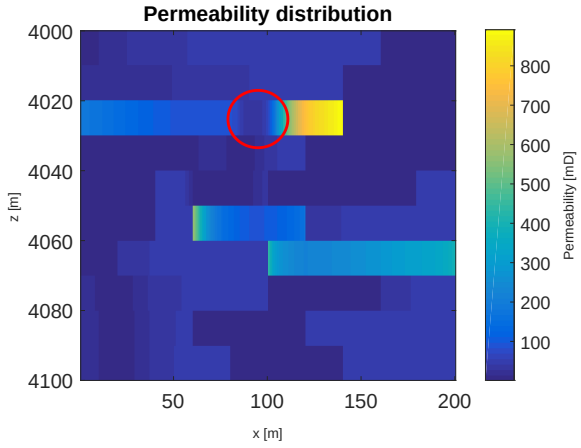

Figure 17 *Permeability K_x at the end of the IDD strategy. The red circle indicates the plug position.*

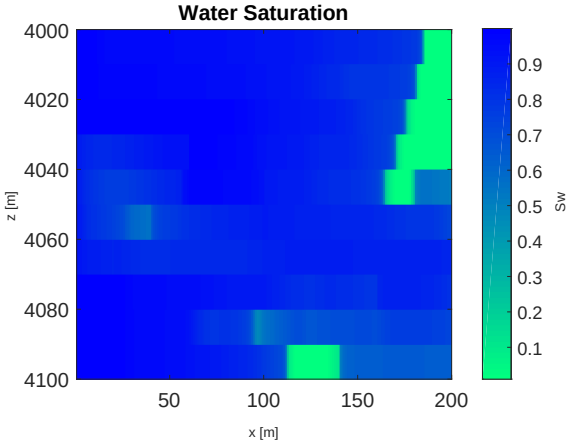

Figure 18 *Water saturation at the end of the IDD strategy.*

Figure 18 shows that less oil is left behind than in the base waterflood case without sodium silicate injection (Figure 16). Oil production is identical for most of the first 520 days in the case with and without silicate solution injection, as indicated by the solid and dashed lines in Figure 19 and Figure 20 respectively. After this period, an increase in oil production and a decrease in water production can be clearly observed.

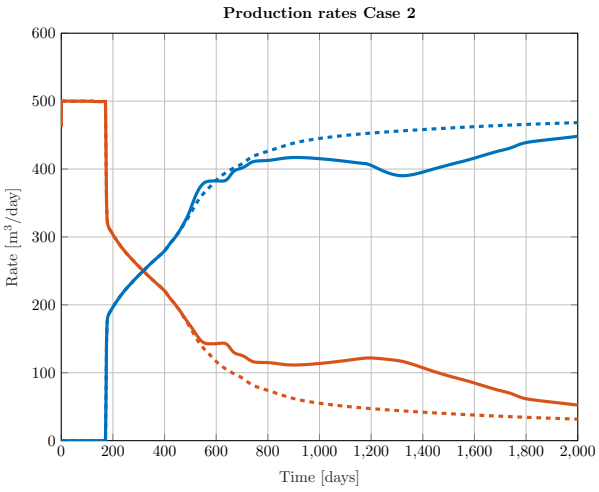

Figure 19 *Oil rate (red) and water rate (blue). With silicate (solid) and without (dashed).*

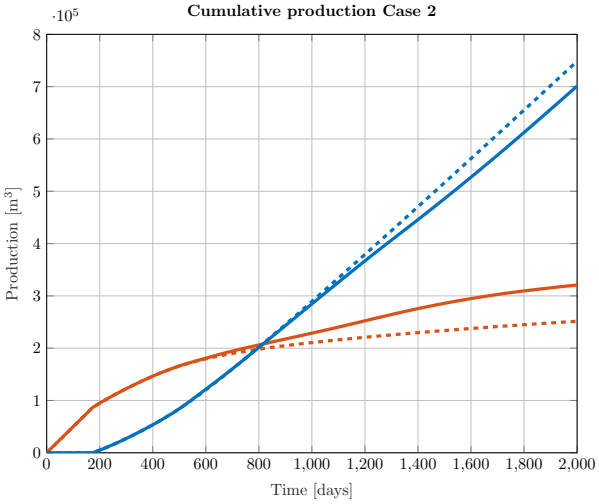

Figure 20 *Cumulative oil rate (red) and water rate (blue). With silicate (solid) and without (dashed).*

The starting control values for the optimization were $[t, \Delta t, C] = [1, 0, 0]$, which corresponds to a waterflood without silicate injection. The bounds for the controls were set to $t \in [1, 2000]$, $\Delta t \in [1, 1000]$ and $C \in [0, 10]$. It took 13 iterations to reach the optimum (Figure 21). Note, that the intermediate result at iteration 5 suggests that the optimization is close to a local optimum strategy in which the silicate solution is injected from day 1. Further iterations ultimately resulted in a significant increase in objective function by delaying this injection.

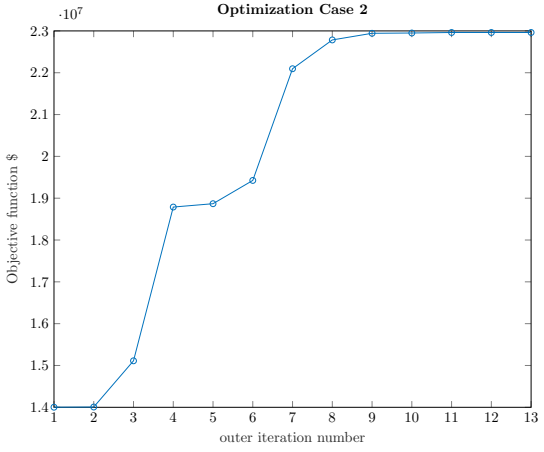

Figure 21 *IDD optimization with $P = 100\ \$/m^3$. Objective function is undiscounted NPV in $.*

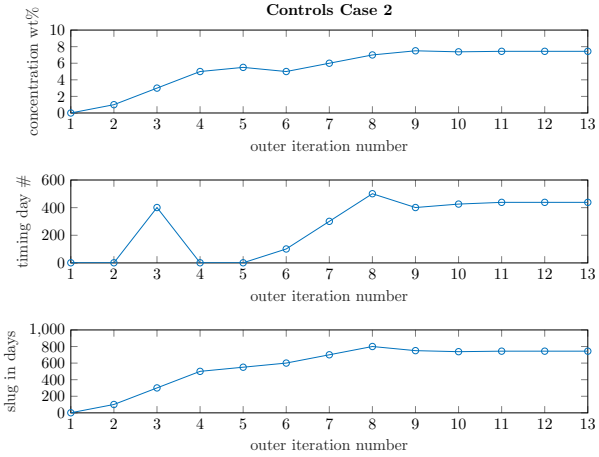

Figure 22 *Control updates during iterations of the Case 2 optimization.*

In order to verify the optimization result, the objective functions values were also evaluated for regular disitributed samples in the control domain, which now has dimension 3 (Figure 23). The optimum is indicated by a red dot. There are small differences in the controls and NPV with the optimum found by optimization. This could suggest a very smooth objective function space with similar NPV for different control combinations.

From the differences with the first optimization case, it is clear that a single operating strategy, optimal for all possible geological scenario's, does not exist for this process. One choice in such case is to optimize the expected recovery or NPV, as evaluated over all available geological realizations.

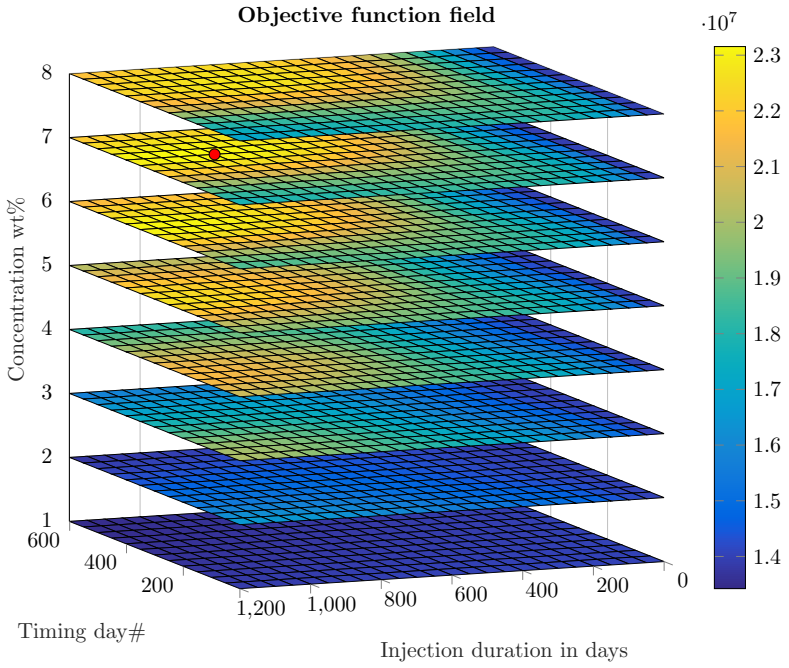

Figure 23 *Objective function values (undiscounted NPV in $.) at regular control intervals. The optimal value is indicated by the red dot.*

Case 3. Robust optimization

In the third case discussed here, it is assumed that geological uncertainty is characterized by an ensemble of 40 equally probable geological models (Figure 25) where the length and position of high permeable paths follow a normal distribution. The initial guess for optimization is $[t, \Delta t, C] = [1, 1, 8]$ (start injection of a 8 wt% solution at day 1 with an injection duration of 1 day). The optimal strategy from the robust optimization is $[t, \Delta t, C] = [482, 379, 6.41]$. The expected objective function value resulting from this optimal strategy is 21.3 million USD, which represents an increase of 40% over the initial strategy.

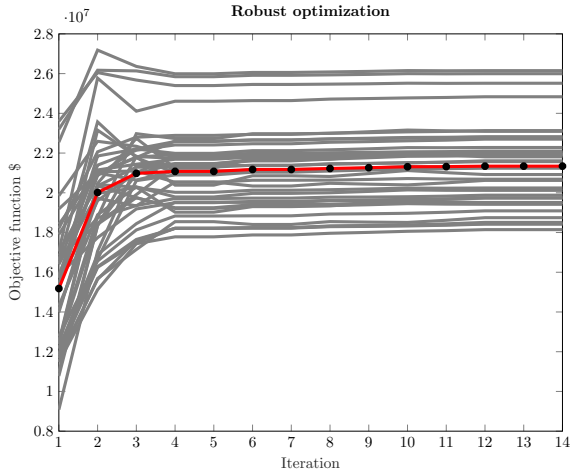

Figure 24 *Robust optimization process for an ensemble of 40 of model realizations. Grey lines indicate individual ensemble members, and the red line represents the ensemble mean.*

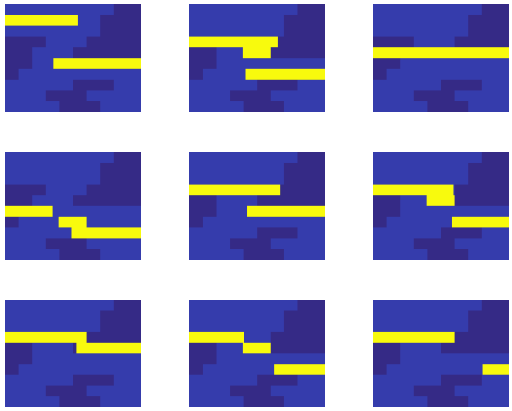

Figure 25 *Nine arbitrary permeability models taken from the ensemble of 40 model realizations.*

Conclusions

We have implemented a fully coupled model to simulate the in-depth diversion (IDD) process. In this study, we proposed the application of an ensemble-based gradient methodology. A simple 2D layered model was used to test our workflow for IDD optimization. A reasonable reactive approach where sodium silicate injection starts just after water breakthrough showed incremental oil production over a base case strategy, defined as a conventional waterflood without implementation of sodium silicate injection.

We observed a limited sensitivity to both spatial and temporal resolution in a simple 2D setting. An increase in relative error in oil production was observed around time of water breakthrough and towards the end of the production period, however rate errors are relatively moderate in absolute terms and the highest relative errors occur when absolute rates are low. Sensitivity of oil recovery and permeability reduction to spatial and temporal resolution confirmed that this observation does not strongly affect total recovery. We conclude that a relatively coarse grid and relatively large time step are acceptable for forward simulation. This may be different in more complex and more heterogeneous cases.

Optimization of the IDD process resulted in improved objective function values, using injection timing, injection duration and concentration of the sodium silicate solution as controls. Different models were observed to result in different optimal strategies, which were not self-evident and differ from a typical reactive strategy. Given uncertainty in permeability, robust optimization was able to find an optimal strategy for an ensemble of 40 model realizations. Ensemble optimization therefore proves to be a viable approach to find optimal IDD strategies. The application to larger and geologically more complex cases and extension with well rate and pressure controls is the topic of on-going investigation.

Acknowledgements

We acknowledge the Stanford University Petroleum Research Institute for Reservoir Simulation (SUPRI-B) program for the permission to use ADGPRS in this study.

References

Chen, Y., Oliver, D.S., Zhang, D. et al. [2009] Efficient ensemble-based closed-loop production optimization. *SPE Journal*, **14**(04), 634–645.

Farshidi, S., Fan, Y., Durlofsky, L. and Tchelepe, H.A. [2013] Chemical Reaction modeling in a compositional reservoir simulation framework. *SPE 163677*.

Fonseca, R., Stordal, A., Leeuwenburgh, O., Van den Hof, P. and Jansen, J.D. [2014] Robust ensemble-based multi-objective optimization. In: *ECMOR XIV-14th European conference on the mathematics of oil recovery*.

Fonseca, R.R.M., Chen, B., Jansen, J.D. and Reynolds, A. [2017] A stochastic simplex approximate gradient (StoSAG) for optimization under uncertainty. *International Journal for Numerical Methods in Engineering*, **109**(13), 1756–1776.

Garipov, T., Tomin, P., Rin, R., Voskov, D. and Tchelepi, H. [2018] Unified Thermo-Compositional-Mechanical Framework for Reservoir Simulation. *Computational Geosciences*.

Hamouda, A.A. and Amiri, H.A.A. [2014] Factors affecting alkaline sodium silicate gelation for in-depth reservoir profile modification. *Energies*, **7**(2), 568–590.

Hatzignatiou, D.G., Giske, N.H. et al. [2016] Water-Soluble Sodium Silicate Gelants for Water Management in Naturally Fractured Carbonate Reservoirs. In: *SPE Europec featured at 78th EAGE Conference and Exhibition*. Society of Petroleum Engineers.

Hiorth, A., Sagen, J., Lohne, A., Nossen, J., Vinningland, J., Jettestuen, E. and Sira, T. [2016] IORSim-A Simulator for Fast and Accurate Simulation of Multi-phase Geochemical Interactions at the Field Scale. In: *ECMOR XV-15th European Conference on the Mathematics of Oil Recovery*.

Icopini, G.A., Brantley, S.L. and Heaney, P.J. [2005] Kinetics of silica oligomerization and nanocolloid formation as a function of pH and ionic strength at 25 C. *Geochimica et Cosmochimica Acta*, **69**(2), 293–303.

Mayer, E., Berg, R., Carmichael, J., Weinbrandt, R. et al. [1983] Alkaline injection for enhanced oil recovery-A status report. *Journal of Petroleum Technology*, **35**(01), 209–221.

Skrettingland, K., Dale, E.I., Stenerud, V.R., Lambertsen, A.M., Nordaas Kulkarni, K., Fevang, O., Stavland, A. et al. [2014] Snorre In-depth Water Diversion Using Sodium Silicate-Large Scale Inter-well Field Pilot. In: *SPE EOR Conference at Oil and Gas West Asia*. Society of Petroleum Engineers.

Skrettingland, K., Giske, N.H., Johnsen, J.H., Stavland, A. et al. [2012] Snorre in-depth water diversion using sodium silicate-single well injection pilot. In: *SPE Improved Oil Recovery Symposium*. Society of Petroleum Engineers.

Stavland, A., Jonsbråten, H., Vikane, O., Skrettingland, K. and Fischer, H. [2011] In-depth water diversion using sodium silicate–Preparation for single well field pilot on Snorre. In: *IOR 2011-16th European Symposium on Improved Oil Recovery*.

Trujillo, R. [2017] *In-depth water diversion strategies*. Msc thesis, Delft Univeristy of Technology.

Trujillo, R., Voskov, D. and Leeuwenburgh, O. [2018] Simulation of In-depth Water Diversion Using Sodium Silicate. In: *43rd Workshop on Geothermal Reservoir Engineering*.

Voskov, D.V., Henley, H. and Lucia, A. [2017] Fully compositional multi-scale reservoir simulation of various CO2 sequestration mechanisms. *Computers and Chemical Engineering*, **96**, 183 – 195.

Voskov, D.V. and Tchelepi, H.A. [2012] Comparison of nonlinear formulations for two-phase multi-component EoS based simulation. *Journal of Petroleum Science and Engineering*, **82**, 101–111.

Zaydullin, R., Voskov, D., James, S., Henley, H. and Lucia, A. [2014] Fully compositional and thermal reservoir simulation. *Computers & Chemical Engineering*, **63**, 51–65.